Catalysis Science & Technology

ROYAL SOCIETY OF CHEMISTRY

PAPER

View Article Online
View Journal | View Issue

Cite this: *Catal. Sci. Technol.*, 2024, 14, 5375

Fluorescence-based pH-shift assay with wide application scope for high-throughput determination of enzymatic activity in enzyme mining and engineering†‡

Avinash Vellore Sunder, Marie-Luise Reif and Wolf-Dieter Fessner *

A number of enzymes important for biocatalyst development or as drug targets are associated with a pH shift during their catalytic reaction, owing to the concommitant release or uptake of protons. Here, we show that an enzyme assay developed using the fluorescent pH indicator HPTS can be adapted for reliable and continuous activity determination of representative enzymes from multiple EC classes that operate in the viable pH range 5.5–8.5, using ratiometric measurement (F_{485}/F_{405}). Kinetic measurements obtained with this method closely match literature values determined using other assay types. Further, the assay was employed to screen variants of transketolase from *Geobacillus stearothermophilus* (TK_{gst}) aimed at engineering substrate promiscuity and remote enantioselectivity for 3-hydroxyaldehydes. The fluorescence-based assay displayed 70-fold improved sensitivity in comparison to an absorption-based assay for transketolase screening, with a limit of detection of 0.044 mM and *Z*-factor of 0.52. Double-site mutagenesis at the G264 and S385 positions yielded variants with 5–15-fold increased activity on the tested 3-hydroxyaldehydes compared to the TK_{gst} (L382F) base variant. Although the directed evolution engineering strategy did not achieve significant remote enantioselectivity in this first round of mutagenesis, the simple fluorescence-based pH-shift assay was shown to be useful as a versatile primary high-throughput screen for *in vitro* enzyme engineering.

Received 1st May 2024,
Accepted 3rd July 2024

DOI: 10.1039/d4cy00566j

rsc.li/catalysis

Introduction

Monitoring enzyme activity is of fundamental importance in enabling drug development and accelerating industrial biocatalysis.[1] Activity assays play an important role in facilitating the discovery of new enzymes, profiling substrate or inhibitor scope, and rapid screening of directed evolution libraries to identify improved enzyme variants.[2] It is therefore essential to develop simple and convenient methods that enable continuous monitoring of enzyme activity with high-throughput parallelization.[3] In particular, a generic assay principle can facilitate application of the assay to a wide range of enzymes and alternative substrates. Several enzymatic reactions are accompanied by the release or uptake of protons, thereby leading to a change in pH of the reaction medium.[4] The use of a pH indicator in a weakly buffered reaction medium therefore offers a rapid and convenient means of monitoring enzyme activity continuously by using a general-purpose pH-shift assay. Most importantly, employing such a generic chemical reaction principle for analysis uncouples the assay from structural requirements concerning the substrate/product or inhibitor, thereby allowing the direct use of unmodified native probes for the screening of enzyme variants.[2] Indeed, several reports have detailed the development of pH-shift assays to monitor the activity of esterases,[5] lipases,[6] nitrilases,[7] dehalogenases,[8] decarboxylases,[9] transketolases,[10] kinases,[11] nucleotidyl-,[12] and glycosyltransferases[13] in the presence of colorimetric pH indicators.

However, fluorescence-based methods allow for lower background, higher sensitivity and greater dynamic range of an assay in comparison to conventional absorption measurements.[14] Development of an intensive signal can be achieved despite a low concentration of the fluorescent dye, yet from very low substrate conversion under initial rate conditions where enzyme activity is usually measured.[15] In a recent report, a derivative of the fluorescent pH indicator 8-hydroxypyrene-1,3,6-trisulfonate (HPTS, pyranine) has been employed in the determination of activity of haloalkane dehalogenases.[16] HPTS has several favourable properties including a high fluorescence quantum yield, dual excitation

Department of Organic Chemistry & Biochemistry, Technical University of Darmstadt, Peter-Grünberg-Straße 4, 64287 Darmstadt, Germany.
E-mail: fessner@tu-darmstadt.de

† Electronic supplementary information (ESI) available. See DOI: https://doi.org/10.1039/d4cy00566j

‡ Dedicated to George M. Whitesides on the occurrence of his 85th anniversary.

nature facilitating ratiometric measurements, and pH sensitivity in the near neutral region,[17] which makes it attractive for the development of a generic enzyme assay system (Scheme 1).

Therefore, in this study we have evaluated the suitability of HPTS as a general fluorescence indicator in pH-shift assays for the rapid quantitative activity determination of several representative enzymes from different EC classes, including esterase, decarboxylase, kinase, nucleotidyltransferase, and glycosyltransferase. In particular, we have focused on transketolase, a thiamine diphosphate (ThDP) dependent enzyme involved in carboligation of aldehyde substrates.[18] *In vivo*, transketolases catalyse the reversible transfer of a 2-carbon hydroxyacetyl unit from a donor ketose sugar phosphate to an acceptor aldose phosphate.[19] However, they have garnered significant attention in synthetic biocatalysis in recent years with respect to their broad substrate scope. Transketolases from *E. coli* or *Geobacillus stearothermophilus* (TK_{gst}) have been modified by semi-rational engineering to facilitate the binding of non-hydroxylated aliphatic[20,21] and aromatic aldehydes,[22,23] stereoinverted 2-hydroxyaldehydes,[24] and diastereomeric aldoses[25] for carboligation by using hydroxypyruvate as a carbonyl donor to drive an irreversible conversion. Transketolases have also been engineered for acceptance of alternative carbonyl donors such as pyruvate[26] or non-native acceptors such as nitrosoarenes.[27] In this context, we have herewith evaluated the alternative fluorescent pH-shift assay with HPTS in high-throughput screening format to screen a small TK_{gst} mutagenesis library against chiral 3-hydroxyaldehydes in an attempt to further engineer substrate promiscuity and remote enantioselectivity.

Results and discussion

Use of a fluorescent pH indicator to measure enzyme activity

The estimation of enzyme activity by measuring a pH shift during the catalytic reaction requires the use of a sensitive and facile pH indicator. Most enzymes relevant for preparative applications are active under neutral to slightly alkaline physiological conditions (pH 7.0–8.5), and the quantification of reaction progress requires dyes with compatible pK_α for optimal sensitivity. In addition, fluorescence measurements offer better dynamic range and sensitivity with low background as compared to reading absorbance. HPTS is a fluorescent pH indicator that has been extensively applied in the preparation of immobilized pH sensors.[28] Besides being inexpensive, non-toxic, and water soluble, HPTS displays a very high quantum yield and photostability. The two excitation maxima of HPTS at λ = 405 and 450 nm facilitate ratiometric measurements, with emission in the fluorescein range allowing the use of a basic filter set for readout. More importantly, the pH sensitivity range of HPTS matches that of HEPES buffer (6.8–8.2), allowing the use of a single indicator/buffer system for application to multiple enzymes that operate within this pH range. Indeed, the use of a HPTS derivative has been recently demonstrated in the measurement of haloalkane dehalogenase activity.[16] Although other fluorescent indicators are commercially available or have been synthesized,[29] these are either expensive, limited to an acidic pH range or show poor water-solubility and quantum yield when compared to HPTS. Although we observed that fluorescent dyes like carboxyfluorescein or 4-methylumbelliferone were also suitable to monitor enzyme activity in the desired pH range, they did not lead to significant change in fluorescence intensity nor offered the advantage of ratiometric measurement (data not shown). We therefore attempted to extend the utility of HPTS to enable the development of a general-purpose assay suitable for activity measurement in multiple enzyme classes.

The presence of three sulfonate groups makes the pK_α of HPTS dependent on the chemical composition of the molecular environment and the ionic strength (IS).[17] In our measurements in HEPES buffer (pH 5.5–9.5), the pK_α of HPTS was determined to be 7.46 at 30 mM IS (Fig. 1), which matches that of HEPES buffer (pK_α 7.48 at 25 °C). This can be easily maintained in the enzyme assay either by adjusting the concentration of required cofactors (*e.g.*, $MgCl_2$ or NTPs) or the addition of NaCl. At 100 mM IS the HPTS pK_α decreased to 7.26 (at 25 °C), in which case MOPS buffer (pK_α 7.2 at 25 °C) could be used to measure enzyme activity, extending the usable pH range for the assay.

Further, the change in HPTS pK_α upon temperature increase to 37 °C closely followed the change in buffer pK_α, confirming that the assay can be utilized in the biologically relevant temperature range. Interestingly, we observed that increase in HPTS concentration from 0.4 to 40 μM in 20 mM HEPES buffer of uniform IS did not significantly alter its pK_α. This is in contrast to a previous report,[16] where the pK_α of soluble HPTS was found to change with increased dye concentration (up to 380 μM in phosphate buffer; however, we did not check such rather high concentrations), while immobilized or ion-paired HPTS did not show altered pH sensitivity.[16]

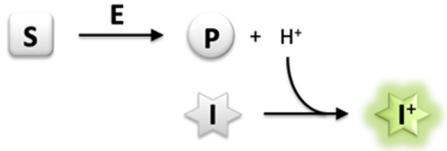

Scheme 1 Generic principle of a pH-shift assay; exemplary illustration for dissociable product formation (S, substrate; E, enzyme; P, product; I, pH-responsive indicator dye).

Transketolase activity and substrate scope

We initially investigated the assay protocol to monitor the progress of the transketolase reaction in an attempt to improve the sensitivity of the established chromogenic assay, which is based on phenol red as an indicator dye. The use of hydroxypyruvate (HPA) as ketol donor with glycolaldehyde as the most reactive acceptor in the TK catalytic reaction

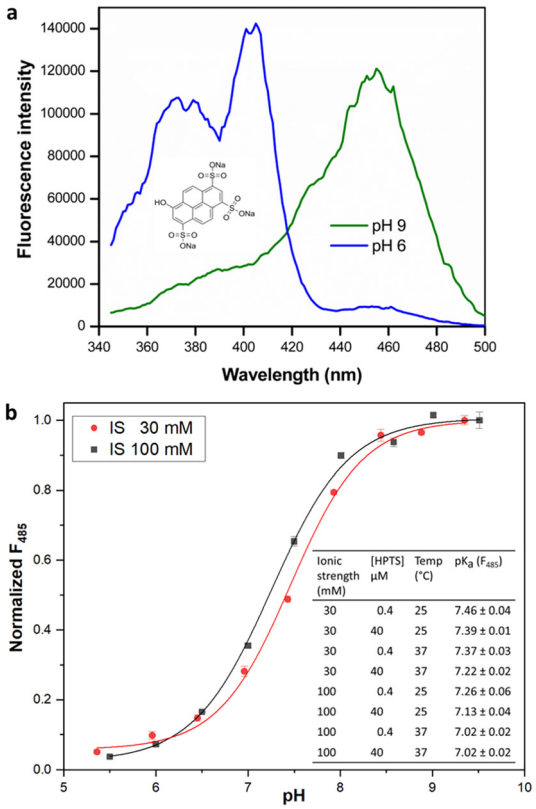

Fig. 1 (a) HPTS structure (inset) and fluorescence excitation spectra, λ_{em} = 511 nm. (b) Dependence of fluorescence intensity (485 nm) of HPTS on pH at 25 °C. Inset: pK_α estimates for HPTS under different reaction conditions. Fluorescence measurements were made as described in methods. pK_α values are given as mean ± SD (n = 3).

releases CO_2, in turn leading to an increase in pH that allows the continuous measurement of TK activity.[10] Because CO_2 is involved in an equilibrium with bicarbonate, and the corresponding partial consumption of hydroxide causes a damped response, this rendered a sensitive fluorescent signal more attractive. A buffer concentration of 2 mM HEPES was used as the reaction medium to provide a balance between sensitivity and accuracy. The starting pH was set at 7.0, as TK_{gst} can maintain maximum activity over a broad pH range (7–8).[30] The enzyme reaction with glycolaldehyde as the model acceptor showed a significant increase in fluorescence intensity ratio (λ_{ex} 485 nm/λ_{ex} 405 nm) over time, compared to blanks with substrate or enzyme omitted (Fig. 2). A slight increase (2%) in signal intensity was observed in the control measurements compared to those with only buffer, which could be attributed to slow thermal degradation of hydroxypyruvate in HEPES buffer.[30] The assay calibration curve (Fig. 2) showed good linearity over 0–1 mM HCO_3^-, and was used to calculate the increase in HCO_3^- concentration over the course of the enzyme reaction. Extrapolation gave a specific activity of 6.11 U mg^{-1} with 20 mM glycolaldehyde (Table 1), which was in good agreement with values obtained from the earlier colorimetric pH assay utilizing phenol red in 2 mM TEA buffer.[10,23] The limit of detection (LOD) and limit

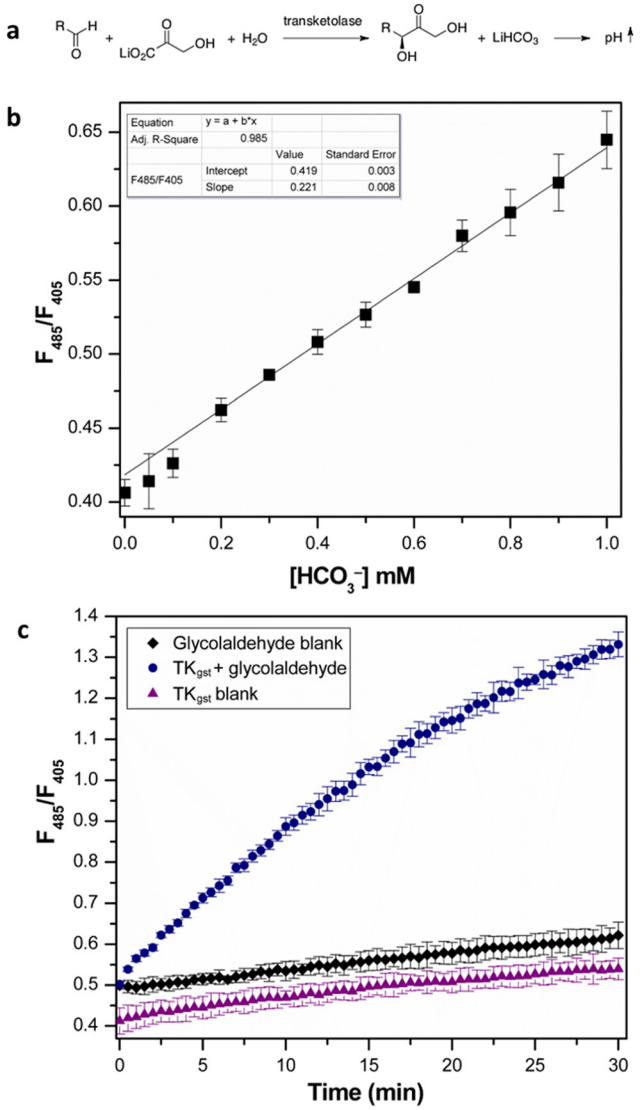

Fig. 2 (a) Transketolase reaction with pH shift. (b) Calibration curve of fluorescence intensity ratio (λ_{ex} 485 nm/(λ_{ex} 405 nm) with $NaHCO_3$ standard (0–1 mM). All measurements were performed in triplicate. (c) Progress of transketolase reaction with 20 mM glycolaldehyde and 50 mM LiHPA. Error bars represent SD from triplicate measurements.

of quantification (LOQ) values derived from the calibration curve were 0.044 and 0.14 mM HCO_3^-, respectively. These are

Table 1 Transketolase (wild-type TK_{gst}) substrate specificity. Activity values are given as mean ± SD from triplicate assays

Aldehyde acceptor	[S] (mM)	TK_{gst} (µg)	Specific activity (U mg^{-1})
Glycolaldehyde	20	4.8	6.11 ± 0.20
D-Glyceraldehyde	20	12	5.14 ± 0.06
D-Lactaldehyde	20	27	0.63 ± 0.02
D-Erythrose	50	27	0.76 ± 0.03
D-Ribose	200	54	0.37 ± 0.005
Propanal	200	54	0.63 ± 0.005
4-Hydroxybutanal	200	81	0.12 ± 0.002
rac-3-Hydroxybutanal	20	54	0.18 ± 0.004
L-Glyceraldehyde	20	81	0.10 ± 0.003

Table 2 Specific activities of different enzymes measured by the fluorescent pH assay. Activity and K_M values are presented as mean ± SD from triplicate assays

Enzyme[a]	EC class	Fluorimetric pH-shift assay conditions[b]	Specific activity (U mg^{-1})	Absorption assay reference[c]	Specific activity[d] (U mg^{-1})	Ref.
Transketolase (*Geobacillus stearothermophilus*)	EC 2.2.1.1	2 mM HEPES pH 7.0 25 °C	6.1 ± 0.1	pH assay (phenol red, 2 mM TEA, pH 7.5)	4.4 ± 0.2	10
				pH assay (phenol red, 2 mM TEA, pH 7.0)	5.8 ± 0.2	
Hexokinase (*Saccharomyces cerevisiae*)	EC 2.7.1.1	2 mM HEPES pH 8.2 25 °C	28.7 ± 1.2	G6PDH coupled assay (NADH oxidation)	25[e]	11
Acetylcholinesterase (electric eel)	EC 3.1.1.7	2 mM HEPES 30 mM NaCl pH 8.0 37 °C	1530 ± 110	Ellman's assay	1527[e]	—
Pyruvate decarboxylase (*Zymobacter palmae*)	EC 4.1.1.1	2 mM MOPS 100 mM NaCl pH 6.5 25 °C	26.1 ± 0.4 K_M = 1.85 ± 0.02 mM	ADH coupled assay	19.2 ± 0.2 K_M = 2.5 ± 0.2 mM	31
N-Acylneuraminate cytidylyltransferase (*Neisseria meningitidis*)	EC 2.7.7.43	2 mM HEPES pH 8.2 37 °C	29.1 ± 2.5	pH assay (cresol red, 2 mM Tris, pH 8.6)	32.6 ± 2.7	12
2,3-Sialyl transferase[f] (*Photobacterium phosphoreum*)	EC 2.4.99.6	2 mM HEPES 30 mM NaCl pH 8.0 30 °C	2.6 ± 0.1 (transferase) 1.4 ± 0.07 (hydrolysis)	pH assay (phenol red, 2 mM Tris, pH 8.0)	1.9 ± 0.03 (5 mM lactose) 1.03 ± 0.02 (hydrolysis)	13

[a] Enzyme was expressed in *E. coli* with C-terminal His tag as described in ESI† and desalted or diluted into the corresponding buffer before assay. [b] Details of substrate and cofactors in the assay mixture are included in text and in ESI.† [c] Other components and conditions were used as mentioned in literature. [d] Specific activity was measured using the reference assays for enzyme preparations that were produced and purified in our lab. [e] Specific activity as specified in product information of commercial lyophilized enzyme preparations obtained from Merck (Sigma-Aldrich; Germany). No reference assays were performed for hexokinase and AChE. [f] Activity was measured in the absence (CMP-Neu5Ac hydrolysis) or presence (sialyl transfer) of 5 mM lactose in the catalytic reaction.

comparable to the corresponding values of 0.04 and 0.11 mM HCO_3^- obtained with 28 μM phenol red.[10] The higher susceptibility, and lower interference from background effects, of the fluorimetric measurement allows reducing the dye concentration (0.4 μM) significantly, which provides adequate sensitivity with a 70-fold lower concentration of indicator compared to the colorimetric assay using phenol red (28 μM).

Next, we used the assay to determine the substrate scope and specific activity of wt TK_{gst} against a set of aldehyde acceptors with varying hydroxylation (Table 1). As expected from its natural specificity, TK_{gst} showed a preference for (2*R*)-hydroxylated aldehydes. The highest activity was observed with glycolaldehyde and D-glyceraldehyde, and significantly lower activity with L-glyceraldehyde. The quantitative activity data obtained using the fluorescent pH assay were similar to those from earlier reports.[23,30] TK_{gst} showed lower activity (5–10% relative to glycolaldehyde) with poly-hydroxylated sugars such as D-ribose and D-erythrose and aliphatic aldehydes such as propanal, even at higher substrate concentrations (50–200 mM).

Kinetic constants were also determined for the acceptors D-glyceraldehyde, glycolaldehyde, and donor LiHPA (Table S2†). Respective K_M values of 7.36 mM, 4.5 mM, and 1.8 mM were obtained, which were in conformity with reported values.[25] Although the values for k_{cat} were slightly lower than reported, this can be explained by a difference in purity of the enzyme sample or changes in the reaction environment that could have interfered with the pH measurement.

Versatility of the assay with enzymes from other EC classes

To explore the versatility of the HPTS-based pH assay, we further investigated a broad range of enzymes from different EC classes (Table 2 and Fig. S1†) that have been extensively developed for industrial biocatalysis or pharmaceutical drug development; most of these enzymes are also active in the HTPS relevant 5.5–8.5 pH range.§

Similar to transketolase, the assay fared well in the detection of hexokinase activity on D-glucose, showing good correlation with the coupled assay employing glucose-6-phosphate dehydrogenase and a commercial hexokinase preparation. Hexokinase is a well-studied metabolic kinase that phosphorylates sugars, where the transfer of a phosphate group from ATP to the terminal hydroxyl group is accompanied by the release of a proton. Hexokinase finds application both in the screening of kinase inhibitors and in biocatalysis for the synthesis of sugar phosphates. The

§ Data reported in BRENDA database (https://www.brenda-enzymes.org).

activity of yeast hexokinase on different sugar substrates was examined using the fluorimetric pH assay (Fig. S2†). In conformity with literature reports,[11,32] the enzyme was most active on D-fructose, D-glucose (28.7 U mg^{-1}), and 2-deoxy-D-glucose, with 50% activity on D-mannose (relative to D-glucose) and 15% activity on sucrose.[11] The assay also showed adequate sensitivity to discern a low activity on D-arabinose (0.1 U mg^{-1}).

Acetylcholinesterase is an important representative of hydrolase enzymes, with therapeutic applications in treatment of neurodegenerative disorders.[33] Employing the fluorimetric pH assay, AChE specific activity could be quantified with a detection limit of 5 mU mL^{-1}, using 1 mM acetylcholine chloride as the substrate and acetic acid as the calibration standard (Fig. S3†). The ionic strength of the assay mixture was adjusted by the addition of 30 mM NaCl. Further, using the assay an IC_{50} value of 1.9 μM could be determined for the known AChE inhibitor galantamine hydrobromide,[33] which was similar to reported values.[34] Although the standard Ellman assay uses acetylthiocholine as substrate, we assume comparable AChE specific activity using the fluorimetric assay with acetylcholine (Table 2), because both substrates have been shown to have similar K_M and k_{cat} using microcalorimetric assays.[35] It is therefore evident that the fluorescence assay has good potential for utilization in the screening and identification of kinase and AChE inhibitors.

Similar to kinases, the assay could also be used for other enzymes that catalyse phosphoryl transfer reactions that are important for preparative biocatalysis, such as in the synthesis of oligosaccharides. For instance, CMP-sialate synthetase (CSS) and 2,3-sialyl transferase (SiaT) are employed in the synthesis of sialylated glycoconjugates that are associated with the regulation of several developmental and immunological processes, as well as microbial pathogenesis.[36] In both cases, laborious or discontinuous methods are required to follow the enzyme reaction. However, alternative colorimetric pH-shift assays have been developed recently (using cresol red or phenol red with Tris buffer) that are simple and advantageous for continuous activity measurement of these enzymes.[12,13] Activity measurements using the fluorescent pH assay gave quantitatively comparable values for CSS, 2,3-SiaT from *Photobacterium phosphoreum* (with lactose as acceptor) and mechanistically related sialidase activities (Table 2 and Fig. S4 and S5†).

Yet another enzyme studied was pyruvate decarboxylase (PDC), an enzyme that has been extensively employed in biofuel production as well as carboligation in biocatalytic synthesis.[31] As the majority of PDCs are most active at acidic pH with a significant decrease in activity beyond pH 7.5, MOPS buffer was employed for the assay at a starting pH of 6.5 (Fig. S6†). The ionic strength was adjusted by the inclusion of 100 mM NaCl to match the pK_α of HPTS and buffer. Specific activity and K_M values obtained with pyruvate (Table 2) for the PDC from *Zymobacter palmae* were comparable to measurements made using the alcohol dehydrogenase-coupled assay,[31] attesting to the versatility of the fluorimetric pH assay.

Application of the assay for engineering remote enantioselectivity in TK_{gst}

We further applied the fluorescent assay in the screening of a TK_{gst} variant library in an attempt to engineer selectivity for enantiomers of 3-hydroxyaldehyde acceptors. The carboligation products are deoxysugars having interesting bioactivity,[37] and the resultant structural 1,3-diol motifs are frequently found in various natural products including polyketides.[38] As noted above, transketolases have been engineered to accept aldehyde acceptors structurally lacking or containing a stereoinverted 2-hydroxyl group, but modifying the TK specificity and selectivity on the more remote 3-hydroxyl group has not been studied so far. In the TK_{gst} active site, several amino acid residues that form a channel for substrate entrance to the catalytic core at the ThDP cofactor are highly conserved. These residues (H462, R521, D470, H28, G264, H263, L191, L382, and S385) bind the aldehyde acceptor and position the electrophilic carbonyl group toward a nucleophilic attack. In order to generate a TK variant library for 3-hydroxyaldehydes, we used the L382F variant as the starting template, because it is known to accept aliphatic aldehydes missing a 2-hydroxyl group.[21] The S385 residue particularly interacts with and stabilizes a (3*R*)-configurated hydroxyl moiety in aldose phosphate acceptors *via* hydrogen bonding (Fig. 3). Therefore, we reasoned that a modification at S385 should modify (improve or even cancel) the preference for the (3*R*)-hydroxyl substrate. The G264 residue is situated opposite to S385, and therefore could be modified to serve as a potential complementary hydrogen-bonding donor when attempting to invert the stereoselectivity toward the (3*S*)-hydroxyl configuration. Accordingly, the G264 residue was first mutated to the amino acids Ala, Val or Ser,

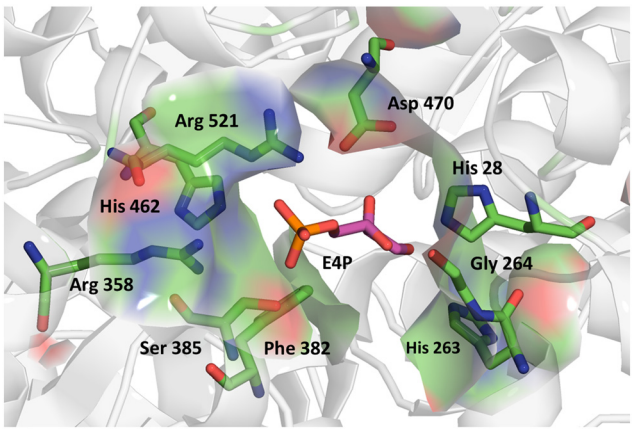

Fig. 3 Acceptor binding site of TK_{gst} L382F with bound erythrose-4-phosphate (purple) illustrating the residues involved in substrate interaction. Structure model was constructed based on the X-ray structure of TK from *Bacillus anthracis* (PDB 3M49). Graphic was produced with PyMOL.[39]

so as to induce a change in substrate orientation without causing steric hindrance for substrate binding. The final TK_{gst} library was generated from the L382F/G264(A,S,V) variants, by mutating S385 using NNK codon degeneracy.

Assays employed to screen enzyme variants generated by directed evolution require adequate sensitivity, reproducibility, robustness, and accuracy, in order to enable fast high-throughput identification of improved hits. The nature of the fluorescent pH assay makes it advantageous as a primary screening technique to discern active variants over a broad substrate range, while also allowing the relatively accurate determination of specific activity, selectivity, or kinetic parameters. To screen the new TK_{gst} variant library, we adapted an optimized method for cell growth in microplates as reported earlier[10] and lysis using only lysozyme and nuclease in 2 mM HEPES buffer. First, the screening protocol was validated using statistic parameters like coefficient of variance (CV) and *Z*-factor.[40] A CV of 14.6% was achieved for the whole process involving cell growth and lysis, protein estimation, and fluorescent assay, with 10.5% CV for the assay alone. A CV value <15% enhances the sensitivity of hit detection by the screening system, allowing identification of variants with at least 2-fold improved activity.[41] We also determined the *Z*-factor by analysing control samples of wild-type TK_{gst} and *E. coli* host with the empty vector, assaying them using 5 mM glycolaldehyde and LiHPA (Fig. S7†). Negligible activity was observed with the *E. coli* background from low expression of its native transketolase. A *Z*-factor of 0.64 was observed for the assay alone and 0.52 for the complete process, which is in the range for an "excellent" assay even with the rate-limiting concentration of glycolaldehyde; implying that the assay fulfils requirements for use in HTS.

Following assay validation, the L382F/G264X/S385X variant library was first subject to preliminary screening to detect variants displaying enhanced activity with 10 mM *rac*-3-hydroxybutanal. While several variants exhibited higher specific activity of up to 5-fold compared to the L382F base variant, a considerable fraction of such variants belonged to the G264V sub-library (Fig. 4). On the other hand, many inactive variants were observed when the G264 residue was either left unchanged or modified to Ala or Ser. Regardless, the top 10% active mutants from each sub-library were chosen and subjected to a second round of screening using 5 mM enantiomerically pure (3*R*)- or (3*S*)-hydroxybutanal (Fig. S8†),[42] with the specific activity ratio used to evaluate potential improvement in enantioselectivity. Unfortunately, significant enhancement in selectivity was not observed, with only 15% of the mutants showing slight improvement in selectivity for (3*S*)-hydroxybutanal (specific activity ratio (*S*/*R*) > 2; Fig. 5a).

It is plausible that 3-hydroxybutanal, being a relatively small and flexible substrate, has a greater freedom of movement in the TK active site, consequently reducing the potential for selective binding of the enantiomers. Similar observations have been made in studies directed at an

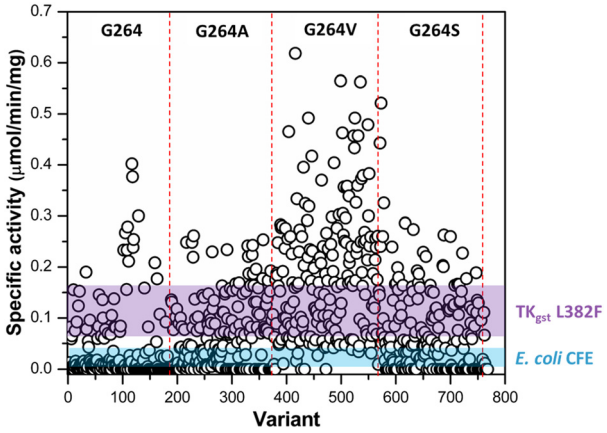

Fig. 4 Preliminary activity screening of TK_{gst} variant library (L382F/G264X/S385X) with *rac*-3-hydroxybutanal. The coloured bands represent mean ± 3SD of the specific activity of TK_{gst} (L382F) mutant and *E. coli* cell-free extract control.

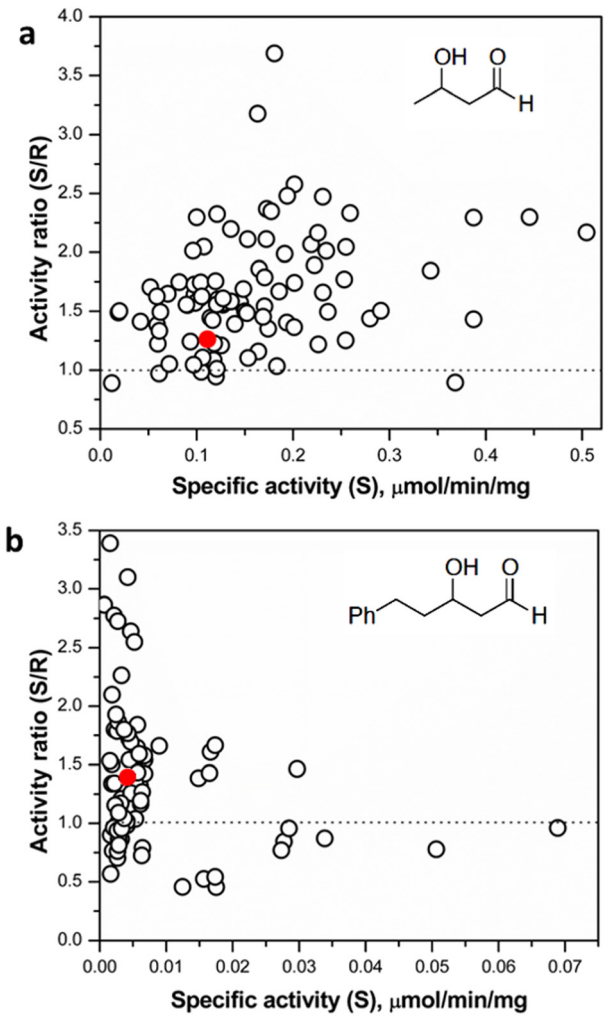

Fig. 5 (a) Screening of selected hits (top 10% active variants from preliminary screening round) with (3*R*)- and (3*S*)-hydroxybutanal. (b) Screening of selected hits with (3*R*)- and (3*S*)-hydroxyphenylpentanal. The red dots denote the reference starting mutant TK_{gst} (L382F).

enantioselectivity switch for 2-hydroxylated aldehydes upon screening libraries with D- or L-glyceraldehyde, which both may productively bind in more than one alternative orientations.[24] The innate low stability of small chain aliphatic aldehydes might also interfere with the measurements. To address this potential lacuna, we further tested the TK_{gst} hit plate against enantiomers of an arylated 3-hydroxyaldehyde (3-hydroxy-5-phenylpentanal, HPP; Fig. 5 and S8†).[43] We hypothesized that the addition of the bulky phenyl moiety should enforce an extended-chain binding orientation of the isomers, thereby improving distinctive substrate–enzyme interactions and thus better discrimination of the 3-hydroxyl configuration. Rescreening of the 3-hydroxybutanal hit plate using the fluorescent assay revealed that HPP indeed was accommodated by 16 variants. The most active variants exhibited up to 15-fold improved activity over TK_{gst} (L382F), indicating that the beneficial effects of G264X/S385X mutations are amplified by the use of a bulky substrate. However, only minor improvement in enantioselectivity was observed even with this substrate, where all the active variants exhibited a specific activity ratio in the range 0.5–3.2 only. Sequencing revealed that the favoured mutations were changes to Ala or Val at both the 264 and 385 positions. The S385V mutation resulted in a slightly higher selectivity for (3*R*)-HPP. An analytical scale reaction using 15 mM *rac*-HPP and the active variant L382F/G264A/S385A (heat-purified enzyme) verified formation of the carboligated adduct according to TLC control (see ESI†).

Although the introduction of remote enantioselectivity could not be successfully completed in this initial study, the mutations at G264 and S385 were able to improve enantiocomplementary binding of 3-hydroxyaldehydes in the active site and their acceptance by transketolase, leading to higher activity. We expect that construction and screening of larger libraries by including further residues with substrate contact should provide enhanced stereoselectivity.

Experimental

Materials and methods

HPTS and aldehyde acceptors for TK were purchased from Sigma-Aldrich, and used freshly as supplied. Hydroxypyruvate (LiHPA) was prepared according to the literature procedure.[44] Enantiomers of 3-hydroxybutanal were synthesized from 4,4-dimethoxybutanone,[42] and 3-hydroxy-5-phenylpentanal from hydrocinnamaldehyde.[43] Transketolase from *Geobacillus thermophilus* (TK_{gst}) was expressed and purified as reported earlier[21] and stored as lyophilized powder until use. Expression and purification protocols for other enzymes used in the study are provided in the ESI.† Fluorescence measurements were performed using a BMG Labtech FLUOstar instrument equipped with 485 nm and 405 nm excitation and 520 nm emission filters. All fluorescence measurements and enzyme assays were performed in 200 μL final volume using flat bottom Nunc Immuno 96-well black microplates.

Characterization of the fluorescent indicator

HPTS fluorescence excitation spectra were measured in 20 mM HEPES buffers of varying pH (5.0–9.5), with emission at 511 nm, on a microtiter plate reader (Infinite F200; Tecan, Crailsheim, Germany). The pH sensitivity of HPTS was determined by measuring fluorescence in 20 mM HEPES buffers of varying pH (5.0–9.5) and constant ionic strength (30 mM or 100 mM). A Knick 761 Calimatic pH meter with a double pore pH electrode calibrated using reference buffers (pH 4.01 and pH 7.00; Carl Roth, Germany) was used for pH measurements. The pK_α values were determined from the inflection point of a sigmoidal fit to fluorescence intensity (485 nm) *versus* pH using Origin 8.5 (OriginLab, USA).

Determination of enzyme activity

For activity determination with pure enzymes, the respective enzyme was desalted into 2 mM buffer of corresponding pH and ionic strength (Table 2, ESI†) before the assay.

TK_{gst} activity. Transketolase assay mixture (200 μL) contained TK_{gst}, aldehyde acceptor (such as 20 mM glycolaldehyde), TPP (2.4 mM), $MgCl_2$ (9 mM) and HPTS (0.4 μM) in 2 mM HEPES buffer pH 7.0. LiHPA (50 mM) was added to start the reaction. The change in fluorescence intensity of HPTS was measured over 30 min at 25 °C. The intensity ratio (485 nm/405 nm) was converted to HCO_3^- concentration using the calibration curve, and specific activity was calculated from the initial linear region.

Assay calibration. Calibration curve was determined by using a series of concentrations of $NaHCO_3$ (0–1 mM) in the reaction mixture containing 12 μg TK_{gst}, but with the aldehyde acceptor omitted. The relationship between product concentration and fluorescence was determined by rationalizing the measured fluorescence (485 nm/405 nm). The limit of detection (LOD) for the assay was measured from deviation and slope of the calibration curve.

Assay mixtures for other enzymes were set up as given in the ESI† and Table 2.

Statistics. All enzyme assays were performed in triplicates and results are expressed as mean ± SD. Assay limit of detection (LOD) was measured as 3.3 × SD/slope from the calibration curve. For evaluation of the assay method for high-throughput screening, *Z*-factor and coefficient of variance (CV) were calculated according to the published method.[40] A total of 48 samples each of wt TK_{gst} and *E. coli* BL21 host cells containing empty plasmid were used for the *Z*-factor calculation.

TK_{gst} variant library construction and screening

Library construction. The TK_{gst} variant library was generated using the L382F mutant as the starting template (for details of primer sequences and PCR conditions see ESI†). The G264 residue was first modified to A, V or S *via* site-directed mutagenesis. The S385 single site saturation library was then created using NNK codon degeneracy with each variant as the base (L382F and L382F/G264A,V,S). 190

colonies were randomly picked from each sub-library (L382F/S385X, G264A/L382F/S385X, G264V/L382F/S385X, and G264S/L382F/S385X) to ensure adequate coverage.

Enzyme expression. The final TK_{gst} variant library (*ca.* 800 clones) was subjected to preliminary screening using the fluorimetric pH assay. For the preparation of enzyme samples, 5 μL from a glycerol stock of each clone was transferred to individual wells in 96-well round bottom microtitre plates containing 130 μL LB growth medium (supplemented with 50 μg mL^{-1} kanamycin). In each plate *E. coli* BL21 (DE3) cells were included as negative control and the TK_{gst} (L382F) variant to measure baseline activity. Plates were covered with sealing foil to avoid evaporation and incubated at 37 °C and 900 rpm shaking for 8–10 h. Then the cultures were transferred (100 μL) from each well to 96-well deep well plates containing 400 μL LB-kan medium with 0.1 mM IPTG. Plates were covered and incubated for 16 h at 30 °C with 1200 rpm shaking. Cells were harvested by centrifugation (2250 × *g* for 30 min at 4 °C) and washed with 2 mM HEPES buffer pH 7.0. Cell lysis was performed in 2 mM HEPES buffer pH 7.0 containing 0.5 mg mL^{-1} lysozyme and 4 U mL^{-1} benzonase (nuclease) at 37 °C for 1 h, followed by incubation at 50 °C for 30 min to enable heat-purification of TK_{gst}.

Library screening. Following centrifugation of cell lysate (2250 × *g* for 30 min at 4 °C), 50 μL of the supernatant was transferred to a new Nunc Immuno black 96-well microplate. To each well, 130 μL substrate solution (10 mM *rac*-3-hydroxybutanal, 9 mM $MgCl_2$, 2.4 mM TPP, 0.4 μM HPTS in 2 mM HEPES at pH 7.0) was added and the reaction was started at 25 °C by the addition of 20 μL LiHPA (final concentration 50 mM). The change in pH accompanying the release of CO_2 during the assay reaction was measured as a function of HPTS fluorescence. The top 10% variants from each G264 sub-library showing higher activity than the TK_{gst} (L382F) control were selected for the next round of screening with individual 5 mM (3*R*)- or (3*S*)-hydroxybutanal isomers, in order to evaluate the enantioselectivity. The same variants were also screened with 5 mM (3*R*)- or (3*S*)-3-hydroxy-5-phenylpentanal isomers, with the addition of 10% DMSO to the assay mixture for substrate solubility. Protein concentration in the cell lysates was measured by means of a bicinchonic acid (BCA) assay kit (ThermoScientific, USA).

Conclusions

The fluorimetric pH-shift assay using HPTS is a practical, efficient and reliable method that can be applied to measure activities of a wide range of enzymes that are important for advanced applications in biocatalysis. Its generic chemical reaction principle renders the assay particularly suitable to evaluate an enzyme's substrate (or inhibitor) scope under consistent reaction conditions. The method is also useful for high-throughput screening of enzyme libraries from enzyme engineering by directed evolution *in vitro* (as demonstrated here for transketolase) or from metagenomic prospecting.

While our results demonstrate its versatility, limitations of the assay include (i) a workable pH range of 5.5–8.5 for direct continuous activity monitoring due to the nature of the pH-shift principle; (ii) a need for measurements at two distinct excitation wavelengths to render a single ratiometric data point, thereby not allowing a direct readout; and (iii) a sensitivity limit when using filter-based plate readers if the available filters do not match the HTPS maxima. However, we expect that these limitations can be tackled with advanced instrumentation and the identification of modified fluorescent dyes having lower or higher pK_α values for use in more acidic or more alkaline ranges, respectively.[17,29] Additionally, the presence of buffering substrates or co-factors, and multiple products that may cause pH changes, may limit the applicability of the assay. Therefore, it is important to maintain uniform starting conditions including pH, temperature, and ionic strength to obtain reliable data from kinetic parameter measurements. Although the assay can be efficiently performed using a standard microtitre plate protocol, we suggest that the high responsiveness and excellent water solubility of HPTS should qualify even as a potential detection system in microfluidic systems for monitoring pH-sensitive reactions under uHTS conditions.

Data availability

The data supporting this article are available within the article and its ESI.†

Author contributions

Avinash Vellore Sunder: investigation, formal analysis, and writing – original draft. Marie-Luise Reif: investigation and formal analysis. Wolf-Dieter Fessner: conceptualization, funding acquisition, formal analysis, supervision, and writing – review and editing.

Conflicts of interest

There are no conflicts to declare.

Dedication

It is with great pleasure that we dedicate this paper to George M. Whitesides on the occurrence of his 85th anniversary. George was my (WDF) postdoctoral advisor from 1986 to 1987 for working on enzymatic asymmetric C–C bond formation by using aldolase catalysis, a topic of major promise for synthetic organic chemistry. After completing my PhD in hardcore hydrocarbon chemistry on realizing the first non-Paquette dodecahedrane synthesis *via* the $C_{20}H_{20}$ isomer "pagodane", the transition to enzyme catalysis in aqueous solution, carbohydrate stereochemistry and sugar phosphate analysis posed quite some challenge. For some years the Whitesides group pioneered the field of enzymatic carboligation with a number of key developments in

Fig. 6 Illustration of "nano-contact printing" technology on the occasion of George M. Whitesides receiving the Emanuel-Merck Lecureship award 2005 at the Technical University of Darmstadt.

asymmetric aldol and acyloin synthesis (*e.g.*, ref. 18), but George's interest soon became captured by other important problems that awaited his fundamental insights and visionary impact. I myself returned to Germany to start my independent research program on enzyme catalysis (guess the topic? *carboligation*!).

Thus, we needed some special reason to get in touch again. At the Technical University of Darmstadt I headed the academic selection committee for the biennial Emanuel-Merck Lectureship Award (**https://en.wikipedia.org/wiki/Emanuel_Merck_Lectureship**) from 2000 to 2022, and George was selected as the recipient of the 2005 award. In my laudatio speech, I addressed many facets of George's impressive achievements, but since the president of our university was attending as well, I then posed the challenge that we at a Technical University should have the courage to do even better engineering work than the ingenious micro-contact printing technology developed by George's group in an academic setting at Harvard. Why not scale down by another order of magnitude: nano-contact printing? In my office I had carved a mirror-image stamp out of a big potato and was therefore able to stamp the letters "NANO" on some index cards using a large ink bath! The problem was solved (Fig. 6), and George played along nicely by kindly hand-signing a few of these cards for us.

Needless to mention that George then presented three excellent award lectures on highly stimulating topics, as diverse as on *microfluidic technology*, *soft lithography*, and *protein ligand design*. Happy Anniversary, George!

Acknowledgements

This project has received funding through The German Federal Ministry of Education and Research (BMBF, grant no. 031B0595) and the initiative ERA CoBioTech (European Union Horizon 2020 Research and Innovation Programme, grant no. 722361). We gratefully acknowledge Alexander Mertsch for help with the synthesis of HPP.

Notes and references

1 S. Slagman and W.-D. Fessner, *Chem. Soc. Rev.*, 2020, **49**, 1968.
2 Y. V. Sheludko and W.-D. Fessner, *Curr. Opin. Struct. Biol.*, 2020, **63**, 123.
3 M. G. Acker and D. S. Auld, *Perspect. Sci.*, 2014, **1**, 56; W.-D. Fessner, *Nat. Catal.*, 2019, **2**, 738; U. Markel, K. D. Essani, V. Besirlioglu, J. Schiffels, W. R. Streit and U. Schwaneberg, *Chem. Soc. Rev.*, 2020, **49**, 233.
4 R. J. Kazlauskas, in: *Enzyme Assays*, ed. J.-L. Reymond, Wiley-VCH, Heidelberg, 2006, pp. 15–39.
5 L. E. Janes, A. C. Löwendahl and R. J. Kazlauskas, *Chem. – Eur. J.*, 1998, **4**, 2324; M. F. Paye, H. B. Rose, J. M. Robbins, D. A. Yunda, S. Cho and A. S. Bommarius, *Anal. Biochem.*, 2018, **549**, 80.
6 F. Morís-Varas, A. Shah, J. Aikens, N. P. Nadkarni, J. Rozzell and D. C. Demirjian, *Bioorg. Med. Chem.*, 1999, **7**, 2183–2188; M. de los Angeles Camacho-Ruiz, J. C. Mateos-Díaz, F. Carrière and J. A. Rodriguez, *J. Lipid Res.*, 2015, **56**, 1057.
7 A. Banerjee, P. Kaul, R. Sharma and U. Banerjee, *J. Biomol. Screening*, 2003, **8**, 559.
8 P. Holloway, J. T. Trevors and H. Lee, *J. Microbiol. Methods*, 1998, **32**, 31; S. Marvanová, Y. Nagata, M. Wimmerová, J. Sýkorová, K. Hynková and J. Damborský, *J. Microbiol. Methods*, 2001, **44**, 149; T. M. Phillips, A. G. Seech, H. Lee and J. T. Trevors, *J. Microbiol. Methods*, 2001, **47**, 181; L. Tang, Y. Li and X. Wang, *J. Biotechnol.*, 2010, **147**, 164.
9 K. Yu, S. Hu, J. Huang and L. H. Mei, *Enzyme Microb. Technol.*, 2011, **49**, 272.
10 D. Yi, T. Devamani, J. Abdoul-Zabar, F. Charmantray, V. Helaine, L. Hecquet and W.-D. Fessner, *ChemBioChem*, 2012, **13**, 2290.
11 E. Chapman and C.-H. Wong, *Bioorg. Med. Chem.*, 2002, **10**, 551.
12 N. He, D. Yi and W.-D. Fessner, *Adv. Synth. Catal.*, 2011, **353**, 2384; D. Yi, N. He, M. Kickstein, J. Metzner, M. Weiß, A. Berry and W.-D. Fessner, *Adv. Synth. Catal.*, 2013, **355**, 3597; A. Mertsch, S. Poschenrieder and W.-D. Fessner, *Adv. Synth. Catal.*, 2020, **362**, 5485.
13 C. Deng and R. R. Chen, *Anal. Biochem.*, 2004, **330**, 219; A. Mertsch, N. He, D. Yi, M. Kickstein and W.-D. Fessner, *Chem. – Eur. J.*, 2020, **26**, 11614.
14 J. R. Lakowicz, *Principles of Fluorescence Spectroscopy*, Springer, New York, 3rd edn, 2006.
15 T. Scheidt, H. Land, M. Anderson, P. Berglund, Y. Chen, D. Yi and W.-D. Fessner, *Adv. Synth. Catal.*, 2015, **357**, 1721; R. Roldán, I. Sanchez-Moreno, T. Scheidt, V. Hélaine, M. Lemaire, T. Parella, P. Clapés, W.-D. Fessner and C. Guérard-Hélaine, *Chem. – Eur. J.*, 2017, **23**, 5005; Y.-C. Thai, A. Szekrenyi, Y. Qi, G. W. Black, S. J. Charnock and W.-D. Fessner, *Bioorg. Med. Chem.*, 2018, **26**, 1320; H. Land, F. Ruggieri, A. Szekrenyi, W.-D. Fessner and P. Berglund, *Adv. Synth. Catal.*, 2020, **362**, 812.
16 S. Nevolova, E. Manaskova, S. Mazurenko, J. Damborsky and Z. Prokop, *Biotechnol. J.*, 2019, **14**, 1800144.

17 O. S. Wolfbeis, E. Furlinger, H. Kroneis and H. Marsoner, *Fresenius' Z. Anal. Chem.*, 1983, **314**, 119; Y. Avnir and Y. Barenholz, *Anal. Biochem.*, 2005, **347**, 34–41; R. Nandi and N. Amdursky, *Acc. Chem. Res.*, 2022, **55**, 2728.
18 D. C. Myles, P. J. Andrulis III and G. M. Whitesides, *Tetrahedron Lett.*, 1991, **32**, 4835; Y. Kobori, D. C. Myles and G. M. Whitesides, *J. Org. Chem.*, 1992, **57**, 5899.
19 G. Schenk, R. G. Duggleby and P. F. Nixon, *Int. J. Biochem. Cell Biol.*, 1998, **30**, 1297.
20 E. G. Hibbert, T. Senussi, M. E. B. Smith, S. J. Costelloe, J. M. Ward, H. C. Hailes and P. A. Dalby, *J. Biotechnol.*, 2008, **134**, 240; J. L. Galman, D. Steadman, S. Bacon, P. Morris, M. E. B. Smith, J. M. Ward, P. A. Dalby and H. C. Hailes, *Chem. Commun.*, 2010, **46**, 7608.
21 D. Yi, T. Saravanan, T. Devamani, F. Charmantray, L. Hecquet and W.-D. Fessner, *Chem. Commun.*, 2015, **51**, 480; C. Zhou, T. Saravanan, M. Lorilliere, D. Wei, F. Charmantray, L. Hecquet, W.-D. Fessner and D. Yi, *ChemBioChem*, 2017, **18**, 455.
22 P. Payongsri, D. Steadman, H. C. Hailes and P. A. Dalby, *Enzyme Microb. Technol.*, 2015, **71**, 45.
23 T. Saravanan, M. L. Reif, D. Yi, M. Lorillière, F. Charmantray, L. Hecquet and W.-D. Fessner, *Green Chem.*, 2017, **19**, 481.
24 J. Abdoul Zabar, M. Lorillière, D. Yi, S. Thangavelu, T. Devamani, L. Nauton, F. Charmantray, V. Hélaine, W.-D. Fessner and L. Hecquet, *Adv. Synth. Catal.*, 2015, **357**, 1715; M. Lorilliere, M. De Sousa, F. Bruna, E. Heuson, T. Gefflaut, V. de Bernardinis, S. Thangavelu, D. Yi, W.-D. Fessner, F. Charmantray and L. Hecquet, *Green Chem.*, 2017, **19**, 425; H. Casajus, A. Lagarde, M. Leremboure, T. D. D. Miguel, L. Nauton, V. Thery, W.-D. Fessner, N. Duguet, F. Charmantray and L. Hecquet, *ChemCatChem*, 2020, **12**, 5772.
25 M. Lorillière, R. Dumoulin, M. L'Enfant, A. Rambourdin, V. Thery, L. Nauton, W.-D. Fessner, F. Charmantray and L. Hecquet, *ACS Catal.*, 2019, **9**, 4754.
26 T. Saravanan, S. Junker, M. Kickstein, S. Hein, M. K. Link, J. Ranglack, S. Witt, M. Lorillière, L. Hecquet and W.-D. Fessner, *Angew. Chem., Int. Ed.*, 2017, **56**, 5358; H. Yu, R. I. Hernández López, D. Steadman, D. Méndez-Sánchez, S. Higson, A. Cázares-Körner, T. D. Sheppard, J. M. Ward, H. C. Hailes and P. A. Dalby, *FEBS J.*, 2020, **287**, 1758; N. Ocal, G. Arbia, A. Lagarde, M. Joly, S. Gittings, K. M. Graham, F. Charmantray and L. Hecquet, *Adv. Synth. Catal.*, 2023, **365**, 78.
27 I. Fúster Fernández, L. Hecquet and W.-D. Fessner, *Adv. Synth. Catal.*, 2022, **364**, 612; I. Fúster Fernández, M. Kickstein and W.-D. Fessner, *Adv. Synth. Catal.*, 2023, **365**, 3861.
28 J. Santner, M. Larsen, A. Kreuzeder and R. N. Glud, *Anal. Chim. Acta*, 2015, **878**, 9.
29 P. Horváth, P. Šebej, D. Kovář, J. Damborský, Z. Prokop and P. Klán, *ACS Omega*, 2019, **4**, 5479.
30 J. Abdoul-Zabar, I. Sorel, V. Hélaine, F. Charmantray, T. Devamani, D. Yi, V. de Berardinis, D. Louis, P. Marlière, W.-D. Fessner and L. Hecquet, *Adv. Synth. Catal.*, 2013, **355**, 116.
31 D. Gocke, T. Graf, H. Brosi, I. Frindi-Wosch, L. Walter, M. Müller and M. Pohl, *J. Mol. Catal. B: Enzym.*, 2009, **61**, 30.
32 A. Sols, G. de la Fuente, C. Villar-Palasi and C. Asensio, *Biochim. Biophys. Acta*, 1958, **30**, 92; H. K. Chenault, R. F. Mandes and K. R. Hornberger, *J. Org. Chem.*, 1997, **62**, 331.
33 J. I. da Silva, M. C. de Moraes, L. C. C. Vieira, A. G. Corrêa, Q. B. Cass and C. L. Cardoso, *J. Pharm. Biomed. Anal.*, 2013, **73**, 44.
34 S. H. Lee, B. C. Kim, J. K. Kim, H. S. Lee, M. Y. Shon and J. H. Park, *Bull. Korean Chem. Soc.*, 2014, **35**, 1681.
35 P. A. A. de Almeida Neves, E. Novato Silva and P. S. L. Beirão, *Adv. Enzyme Res.*, 2017, **5**, 1.
36 S. Dedola, S. Ahmadipour, P. de Andrade, A. N. Baker, A. N. Boshra, S. Chessa, M. I. Gibson, P. J. Hernando, I. M. Ivanova, J. E. Lloyd, M. J. Marın, A. J. Munro-Clark, G. Pergolizzi, S.-J. Richards, I. Ttofi, B. A. Wagstaff and R. A. Field, *RSC Chem. Biol.*, 2024, **5**, 167.
37 C. J. Thibodeaux, C. E. Melançon and H.-W. Liu, *Nature*, 2007, **446**, 1008.
38 C. Hertweck, *Angew. Chem., Int. Ed.*, 2009, **48**, 4688.
39 W. L. DeLano, *The PyMOL Molecular Graphics System, Version 1.3*, Schrodinger LLC, 2002, **https://www.pymol.org**.
40 J. H. Zhang, T. D. Y. Chung and K. R. Oldenburg, *J. Biomol. Screening*, 1999, **4**, 67.
41 O. Salazar and L. Sun, *Methods Mol. Biol.*, 2003, **230**, 85.
42 R. Roldán, K. Hernandez, J. Joglar, J. Bujons, T. Parella, I. Sánchez-Moreno, V. Hélaine, M. Lemaire, C. Guérard-Hélaine, W.-D. Fessner and P. Clapés, *ACS Catal.*, 2018, **8**, 8804.
43 M. Narasimhulu, T. Srikanth Reddy, K. Chinni Mahesh, A. Sai Krishna, J. Venkateswara Rao and Y. Venkateswarlu, *Bioorg. Med. Chem. Lett.*, 2009, **19**, 3125.
44 F. Dickens and D. H. Williamson, *Biochem. J.*, 1958, **68**, 74.

